Low-Temperature Steam Reforming of Raw Bio-Ethanol Over Ceria-Zirconia Supported Catalysts

Vincenzo Palma, Concetta Ruocco*, Antonio Ricca

University of Salerno, D. I. In., Via Giovanni Paolo II 132, 84084 Fisciano (SA), Italy
cruocco@unisa.it

Presently, steam reforming of bio-ethanol is considered as a promising route for generation of H_2-rich mixtures with very low environmental concerns. However, the main challenges of such technology are related to catalyst deactivation due to carbon formation. In fact, bioethanol mixtures, besides water and ethanol, may contain several impurities, including higher alcohols, which decrease catalyst resistance towards coking.
In the present work, ethanol steam reforming was investigated over bimetallic Pt-Ni based catalysts supported on ceria-zirconia. Preliminary tests were carried out under pure water/ethanol mixture and the impact of temperature (400 - 500 °C), space velocity (7,500 - 30,000 h^{-1}) and H_2O/C_2H_5OH molar ratio (3 - 9) on carbon formation rate was studied. Further, at chosen operative conditions, a model mixture containing 1 mol% of the main bioethanol impurities (C_2H_4O, C_3H_7OH, C_4H_9OH, $C_5H_{11}OH$) was fed to the reformer and its effect on catalyst stability was studied at 450 °C, 15,000 h^{-1} and r.a.=6.

1. Introduction

The dependency of energy production form fossil fuels mainly results in the emission of CO_2 and other pollutants in the atmosphere. On the other hand, renewable energy provides a favourable alternative to the problem of greenhouse gases emission. In this scenario, hydrogen produced from biofuels and its use in fuel cells is arousing a great interest. At that end, steam reforming of ethanol has been extensively studied (Moretti et al., 2015). Although its clean nature, there are only few publications on the employment of raw bioethanol mixtures as H_2 source. Bioethanol, produced by hydrolysis and fermentation of a wide variety of agricultural and forestry waste, is an aqueous solution containing different oxygenated compounds (alcohols, acids, aldehydes, etc.). However, the presence of organic impurities in the feed can induce carbon formation rates higher than those measured under pure water/ethanol mixtures (Le Valant et al., 2010 a). In order to avoid the expensive purification processes, the selection of appropriate catalysts is a key issue.

For $MgAl_2O_4$-supported catalysts (Rass-Hansen et al., 2008) tested under a raw mixture containing several impurities (< 1 mol% of isoamyl alcohol, isobutyl alcohol, active amyl alcohol, propanol and other species having lower concentrations), the 10 wt%Ni and K (1 wt%)-Ni samples showed similar carbon formation (especially between 450 and 600 °C) while the employment of Rh (2 wt%) as active species reduced coke selectivity of almost 5 times. A 1wt%Rh/$MgAl_2O_4$/Al_2O_3 catalyst (Le Valant et al., 2011) deactivated (reduction in ethanol conversion of almost 25 %) under a simulated bioethanol mixture containing both linear and branched alcohols. However, this effect was more pronounced in the presence of branched alcohols compared to the linear ones.

Bimetallic formulations were also employed for raw bioethanol reforming. By feeding a mixture containing 1 mol% of methyl-2 propan-1ol, the addition of Ni to a Rh/Y_2O_3-Al_2O_3 catalyst (Le Valant et al., 2010 b) was shown to improve catalyst stability, due to a significant reduction in coke yield (the amount of coke deposit was reduced of almost 3 times). On the other hand, the incorporation of small amounts of Rh (1wt%) on 30wt%Ni/CeO_2-ZrO_2 catalysts enhanced hydrogen selectivity (which passed from 53 to 73 % at 600 °C under a steam to ethanol ratio of 13 and with a co-feeding of 1 mol % of butanediol and glycerol and 0.5 mol% of butandioic and acetic acid) as well as ethanol conversion (Mondal et al., 2015).

The aim of this work is to study the performances of Pt-Ni/CeO₂-ZrO₂ as catalyst for bio-ethanol steam reforming (ESR), with particular attention to the role of contaminants on catalyst stability. In order to verify the catalyst resistance to coking, preliminary tests were performed under pure water/ethanol mixture at different temperatures, space velocity and water contents. Further, the impact of bioethanol impurities on carbon formation was evaluated.

2. Experimental

2.1 Catalyst preparation and characterization

A material with 3 wt%Pt-10wt%Ni/CeO₂-ZrO₂ catalyst was prepared by a wet impregnation method. CeO₂-ZrO₂ support (supplied by Rhodia) was preliminary calcined at 600 °C (10 °C/min) for 3 h. Afterwards, a specific amount of support was added to an aqueous solution of Ni(OCOCH₃)₂*4H₂O (Sigma-Aldrich) and impregnation was carried out on a stirring and heating plate. Then, the sample was dried at 120 °C for 12 h and calcined at the same conditions reported for the bare support. Pt deposition was carried out by the same procedure and PtCl₄, provided by Sigma Aldrich, was employed as salt precursor. The benefits of having platinum at the gas-solid interface in terms of ethanol conversion and coke precursors hydrogenation was highlighted in a previous work (Palma et al.,2012).

The Pt-Ni/CeO₂-ZrO₂ catalyst as well as the bare support were characterized through different techniques. Specific area measurements were carried out through N₂ adsorption at -196 °C, using a Sorptometer 1040 ''Kelvin'' from Costech Analytical Technologies. X-ray diffraction spectra were produced by a D8 Brooker and average crystallites size was calculated by means of Scherrer formula. The effective metal load was determined through the Energy Dispersive X-Ray Fluorescence (EDXRF) analysis (Thermo-Scientific QUANT'X). Temperature programmed reduction (TPR) measurements were carried out in the laboratory apparatus described in Paragraph 2.2. The temperature was increased to 650 °C (20 °C/min); a 5 % H₂ in N₂ flow rate was used as reducing stream, ensuring a GHSV of 150,000 h⁻¹. The carbonaceous deposits formed during the steam reforming of ethanol were analysed by temperature programmed oxidation (TPO) method. TPO measurements were performed under a 5 % O₂ in N₂ stream, at the same conditions reported for TPR analysis, except for the heating rate, which was lower (10 °C/min). Before TPO, catalysts were evacuated from species eventually adsorbed on catalyst surface under 1,000 Ncm³/min of N₂ from room temperature to 650 °C at 10 °C/min.

2.2 Catalytic studies

The catalytic stability for ESR reaction was evaluated between 400 and 500 °C, at atmospheric pressure in a stainless steel fixed bed annular reactor (i.d. = 15 mm, o.d. = 17 mm). 5.6 g of catalyst, crushed and sieved to 45-80 mesh, was packed in the reactor between two quartz flakes. The water/ethanol mixture (0.13 mL/min of C₂H₅OH), stored at the desired molar ratio in a tank under N₂ pressure, was fed to a vaporizer through a mass flow controller (MFC) for liquids provided by Bronkhost and mixed with 650 Ncm³/min (at a space velocity of 15,000 h⁻¹) of N₂, obtained through a MFC supplied by Brooks. All the lines linking the boiler with reaction or analysis section are heated at 140 °C in order to avoid water condensation. The reactor was paced in an electrical oven, controlled by a TLK (TLK 43 by Tecnologic) and the catalytic volume temperature was monitored at the center of the catalyst end section. A system of 5 two-ways heated solenoids allowed the reaction mixture to be send to the reactor or, alternatively, to the analysis section. The product gases distribution was continuously monitored by means of FT-IR spectrophotometer (Nicolet Antaris IGS by Thermo Electron). Moreover, a thermo-conductivity and paramagnetic analyzers (CALDOS 27 and MAGNOS 206 by ABB) were employed to record H₂ and O₂ concentrations, respectively. A sample gas conditioning system, placed between FT-IR and CALDOS /MAGNOS, ensured ABB normal operation.Catalytic tests were preliminary preformed at different operative conditions: temperature ranged between 400 and 500 °C, gas hourly space velocity (GHSV) from 75,000 and 30,000 h⁻¹ and water/ethanol molar ratio (r.a.) varied in the range 3-9. All the tests, if not specified, were carried out by keeping constant both ethanol concentration in the feeding stream (5 %) and catalytic volume. The effect of crude bioethanol impurities on stability of Pt-Ni/CeO₂-ZrO₂ catalyst was studied at T = 450 °C, GHSV = 15,000 h⁻¹ and r.a. =6. The present work was focused on the analysis of the following contaminants: acetaldehyde (C₂H₄O), isopropyl alcohol (C₃H₇OH) iso-butanol (C₄H₉OH) and isoamyl alcohol (C₅H₁₁OH). These species were selected on the basis of the typical composition of a lignocellulosic bioethanol (Styarini et al., 2013). In order to study the impact of each type of impurity on the ethanol steam reforming, ''model'' raw ethanol mixtures were prepared by adding 1 mol % (with respect to ethanol) of the selected impurity. These values, higher than the real ones, were selected in order to better see the effect of each contaminant. The catalytic performances in the different operative conditions were reported in terms of ethanol (X$_{C2H5OH}$) and water conversion (X$_{H2O}$) as well as products selectivities (S$_i$), reported, in Equ(1), (2) and (3); v is the stoichiometric ratio between the reaction product and ethanol. The carbon formation rate (CFR) parameter, defined in Eq(4), is expressed as the ratio between the

coke mass deposited on catalyst surface (m_c), detected through TPO, and the total carbon fed ($m_{c,f}$) during time-on-stream (TOS) tests, normalized with respect to both catalyst mass (m_{cat}) and TOS (t).

$$X_{C_2H_5OH} = \frac{\text{moles } C_2H_5OH,in - \text{moles } C_2H_5OH,out}{\text{moles } C_2H_5OH,in} \qquad (1)$$

$$X_{H_2O} = \frac{\text{moles } H_2O,in - \text{moles } H_2O,out}{\text{moles } H_2O,in} \qquad (2)$$

$$S_i = \frac{\text{moles } product,out}{v * (\text{moles } C_2H_5OH,out - \text{moles } C_2H_5OH,in)} \qquad (3)$$

$$CFR = \frac{m_c}{m_{c,f} * m_{cat} * t} \qquad (4)$$

3. Results and discussion

3.1 Catalysts characterization

Table 1 presents the variation (almost 24 %) in CeO_2-ZrO_2 specific area due to active species deposition. Moreover, for both Pt and Ni, the loading obtained by XRF analysis was close to the nominal one.

Table 1: BET surface area, chemical composition and crystallite sizes of the support and the final catalyst

Sample	SSA (m^2/g)	Pt load (%)	Ni load(%)	d_{CeO2} (Å)	d_{NiO} (Å)
CeO_2-ZrO_2	64	-	-	69	-
Pt-Ni/CeO_2-ZrO_2	49	3.04	10.2	73	166
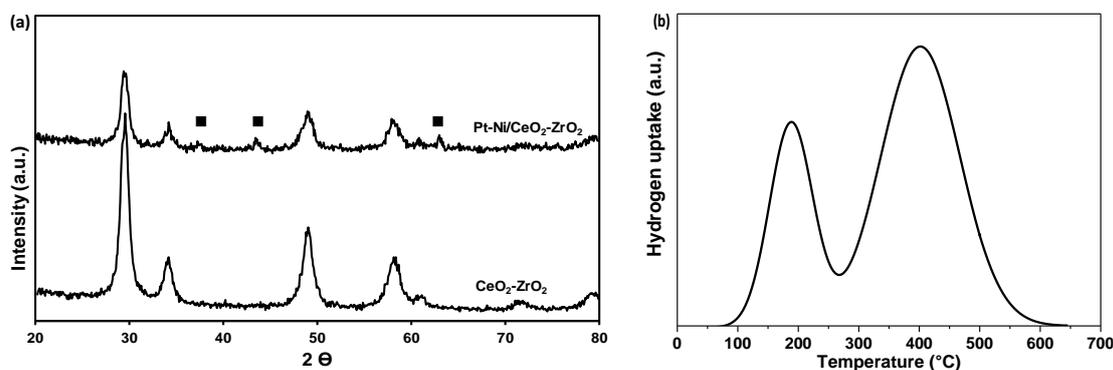
Figure 1: (a) XRD spectra of CeO_2-ZrO_2 and Pt-Ni samples (■ NiO); (b) H_2-uptake profile for the catalyst

Figure 1 (a) displays the X-ray diffraction patterns of the bare support and Pt-Ni/CeO_2-ZrO_2 catalyst. The diffractograms of both the samples exhibited the characteristic displacement in CeO_2 peaks, due to the presence of a ceria-zirconia solid solution (Shao et al., 2014). In addition, cubic crystalline NiO diffraction peaks have been revealed at 37.25, 43.28 and 63.88° (JSPDS No. 47-1049). Conversely, no Pt species diffractions were observed, implying that their crystallite sizes were very small or that platinum oxides are highly dispersed. The crystallite sizes of CeO_2 particles determined by XRD (Table 1) were negligibly affected by active species deposition. Moreover, an average value of 114 Å was measured for NiO crystallites.

Table 2: Hydrogen consumption of TPR profile

Sample	Active species oxide	Peak position (°C)	Theoretical (μmol/g)	Experimental (μmol/g)
Pt-Ni/CeO_2-ZrO_2	PtO_2	188	308	937
	NiO	402	1,704	2,395

As shown in Figure 1(b), the TPR curve of Pt-Ni/CeO_2-ZrO_2 catalyst after deconvolution revealed two hydrogen consumption peaks at 188 and 402 °C. Hydrogen consumption (Table 2) related to the first peak (937 μmol/g_{cat}) was higher than the expected on the basis of Pt content in the catalyst, indicating that NiO and/or surface CeO_2 reduction was promoted by the Pt sites that were being formed upon PtO_x reduction. The broad peak observed at high temperature also comprise the reduction of surface ceria. In fact, the hydrogen consumption is almost 1.5 times higher than the uptake involved in NiO reduction. This phenomenon, known as hydrogen spillover, is widely reported in the literature for rare earth supported metal catalysts (Ay et al.,

2015). Besides, Zr^{4+} incorporation into ceria structure strongly enhances the mobility of lattice oxygen within the solid, thus facilitating the reduction process of the final catalyst.

3.2 Ethanol steam reforming over Pt-Ni/CeO₂-ZrO₂: impact of T, GHSV and r.a. on stability

The operative conditions for stability tests performed under pure H_2O/C_2H_5OH mixtures are reported in Table 3. Total ethanol conversion (not reported) was recorded, whatever the test conditions applied. The increase in reaction temperature from 400 to 500 °C, according to thermodynamic prediction, favorably affected water conversion and methane selectivity, thus resulting in a growth of S_{H2}, which passed from 36.7 % at 400 °C to 63.9 % at 500 °C. However, TPO measurements also revealed a rise in carbon formation rate, especially when T was increased from 450 to 500 °C. Probably, at high temperatures, methane decomposition reaction occurred, which was responsible, on one hand, of H_2 selectivity increase, on the other hand of coke deposition on catalyst surface. Conversely, when the water content in the feeding mixture was higher, beside increasing the steam reforming activity (as attested by S_{H2} and S_{CH4} trends), a more pronounced contribution of coke gasification reaction was assured. As a consequence, lower CFR were measured for r.a. growing from 3 to 9.

Table 3 Operative conditions and results of stability tests carried out without impurities

	Effect of T			Effect of r.a.			Effect of GHSV		
r.a. (-)		6		3	6	9		6	
GHSV (h⁻¹)		15,000			15,000		7,500	15,000	30,000
T (°C)	400	450	500		450			450	
X_{H2O} (%)	17.7	19.2	27.9	29.6	19.2	17.8	26.1	19.2	18.9
S_{H2} (%)	36.7	45.3	63.9	36.1	45.3	54.1	54	45.3	42
S_{CO} (%)	4.67	5.65	13.1	10.4	5.65	5.37	5.92	5.65	3.83
S_{CO2} (%)	52.9	55.4	60.1	47.5	55.4	66.3	60.1	55.4	51
S_{CH4} (%)	42.5	37.1	23.2	46	37.1	27.1	32.4	37.1	40.3
CFR × 10⁵ $g_c/(g_{c,f}*g_{cat}*h)$	0.19	0.33	8.36	2.17	0.33	0.24	0.26	0.33	1.21

The effect of contact time on product gas distribution as well as coke formation tendency of the system was also evaluated. As reported in Table 3, the reduction of contact time caused a lower activity towards steam reforming and a reduced contribution of coke gasification reaction. The latter pathway take place between two phases (steam and solid carbon) and it is generally accepted that the interaction between homogeneous and heterogeneous reactions is very complicated (Sheikh et al., 2015). In fact, the generation as well as the consumption of the species take place at different reaction rates within the fluid as well as on catalyst surface. Commonly, the rate of heterogeneous pathways is lower than that of homogenous reaction. Probably, at a contact time of 120 ms the desired coke removal by steam occurred at lower rates, resulting higher CFR values (Figure 2(b)). The results reported in Table 3 revealed that carbon formation rate is not significantly affect by temperature increase between 400 and 450 °C, space velocity change from 7,500 and 15,000 h⁻¹ and water to ethanol molar ratio growing between 6 and 9. Feeding mixtures with higher water content better simulate the composition of raw bioethanol mixtures. The typical water/ethanol ratio is equal to 20 (Kiss et al., 2012). However, when a H_2O/C_2H_5OH ratio equal to 9 was employed for stability tests, a more difficult management of the laboratory apparatus was observed. Moreover, the heat required for the mixture vaporization increased. Therefore, the effect of crude bioethanol contaminants on bimetallic catalyst performances was carried out at the following operative conditions: r.a. = 6, GHSV = 15,000 h⁻¹ and T = 450 °C.

3.3 Ethanol steam reforming over Pt-Ni/CeO₂-ZrO₂: impact of bioethanol impurities on stability

Model bioethanol mixtures were prepared by adding individually 1 mol % of every impurities and the stability tests were performed for 5 h. No effect of contaminants addition was observed on ethanol conversion, which was total independently from the species added. The results in terms of hydrogen selectivity as well as carbon formation rate as a function of the different impurities are shown in Figure 2 (a) and (b). The presence of contaminants increased H_2 selectivity with respect to the pure water/ethanol mixture case. In particular, a growth in hydrogen production (Figure 2 (a)) was observed with the increase of the number of carbon atoms in the impurity. Likewise, the carbon formation rate (Figure 2 (b)) was also higher than the value measured for the contaminant-free tests and the trend of CFR growth was the same of that observed in H_2 selectivity, except for acetaldehyde. C_2H_4O, in fact, can be de-carbonylated to CH_4 (Romero-Sarria et al., 2008), which, in turn, is responsible for coke formation due to decomposition reaction. The increase of hydrogen selectivity with impurities carbon content ca be explained considering two effects: higher reforming activity (due to the

contribution of contaminants) as well as lower activity towards coke gasification reactions, attested by the growth in carbon formation rate.
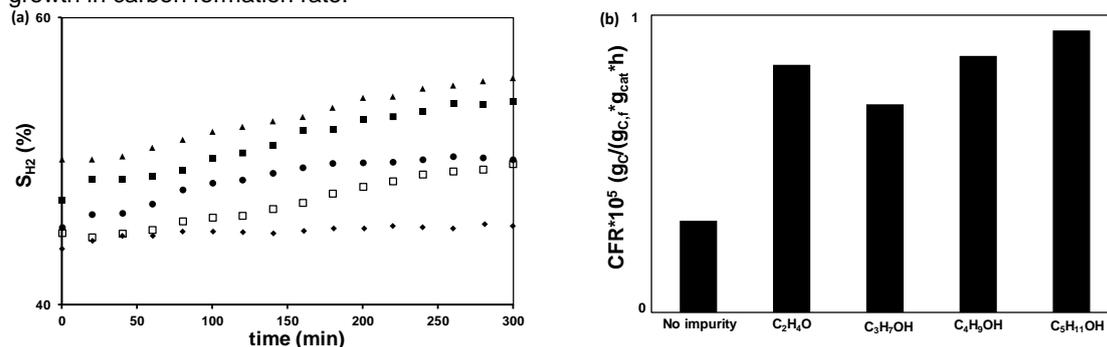
Figure 2: H$_2$ selectivity (a) and carbon formation rate (b) as a function of the impurity; T=450 °C, r.a.=6, GHSV=15,000 h^{-1}. No impurity (filled diamond), C$_3$H$_7$OH (empty square), C$_2$H$_4$O (filled circle), C$_4$H$_9$OH (filled square) and C$_5$H$_{11}$OH (filled triangle)

The Pt-Ni/CeO$_2$-ZrO$_2$ stability was also investigated under a model mixture containing 1 mol % of all the impurities. Total ethanol conversion (not reported) was recorded for almost 24 h of TOS. However, a pronounced variation in product gas distribution (Figure 3 (a)), with a strong reduction in methane selectivity was observed. This effect can be explained by considering that one of the main roles (Jacobs et al., 2007) of Pt during reforming reaction would be to hydrogenate reaction intermediates through methanation reaction. Therefore, it was possible that, during ESR, impurities partially adsorbed on catalyst surface, thus resulting in a partial reduction of Pt hydrogenation capability which led, in turn, to lessened CH$_4$ selectivity.
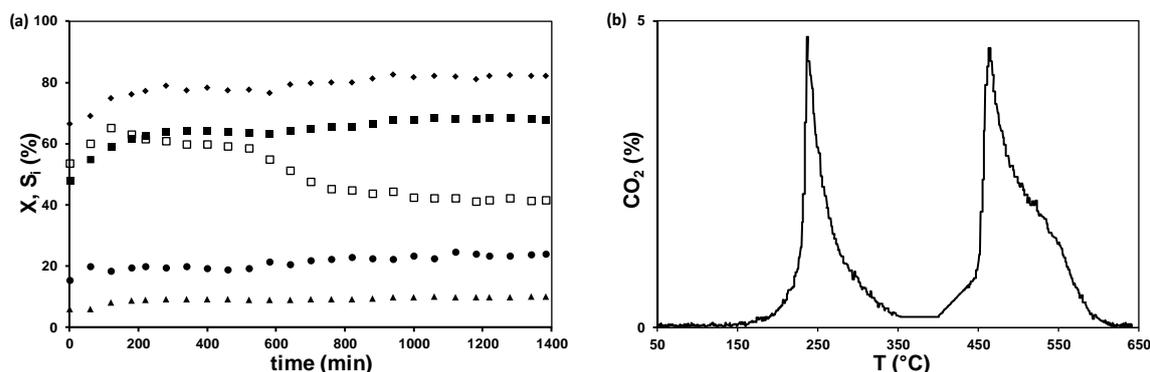
Figure 3: (a)H$_2$O conversion (filled circle) and products selectivities (CO, filled triangle; CH$_4$, empty square; H$_2$, filled square; CO$_2$, diamond) as a function of TOS (1 mol % of every impurity, GHSV=15,000 h^{-1}, T=450 °C, r.a.=6) and (b) typical TPO profile recorded after stability tests (5 % O$_2$ in N$_2$, 1,000 Ncm^3/min)

Figure 3 (b) displays the TPO profile recorded over the Pt-Ni/CeO$_2$-ZrO$_2$ catalyst tested at the conditions reported for Figure 3 (b). Two different types of carbon were observed during the measurement, which correspond to a peak at 250 °C and a broad oxidation zone at higher temperatures. Generally, the oxidation of amorphous coke is observed at T < 350 °C (Koo et al., 2015) while CO$_2$ formation ascribable to more ordered carbonaceous deposits can be seen only at T > 400 °C. In particular, the shoulder peak recorded at 550 °C is probably due to the presence of whisker-type carbon, originated from CH$_4$ decomposition (Zhu. et al., 2015).

In a previous work (Palma et al. 2014), we compared the carbon selectivity of our bimetallic catalysts supported on rare earth oxides with the results found in the recent literature. Very low carbon formation rates were assured by the Pt-Ni catalyst and these results were confirmed also in the presence of the main bioethanol impurities. In fact, at the investigated operative conditions (which, as shown in Table3, displayed intermediate results in terms of coke selectivity), contaminants addition increased carbon formation rate only to 12.5 $\times$·10^{-5} g$_c$/(g$_{c,f}$*g$_{cat}$*h) and such results are still competitive. Moreover, for other studies (Le Valant et al., 2011) focused on the effect of bioethanol impurities, catalyst stability was evaluated for lower TOS; otherwise, ethanol conversions lower than 100 % were recorded during stability tests (Mondal et. al, 2015).

4. Conclusions

In this study, the performance of a bimetallic Pt-Ni/CeO$_2$-ZrO$_2$ catalyst for ethanol steam reforming at low temperature was investigated. The results of tests carried out at different operative conditions in terms of temperature, space velocity and water/ethanol ratio revealed that low temperatures as well as high contact time and r.a. are able to minimize carbon deposition on catalyst surface. Further stability tests were performed by adding 1 mol% of the main bioethanol impurities to pure water/ethanol mixture: whatever the species, total ethanol conversion and a growth in H$_2$ selectivity with the contaminant carbon content was observed. However, a slight increase in carbon formation rate was also measured through TPO analysis. Under a model raw bioethanol mixture containing all the investigated impurities, the selected catalyst displayed high coking resistance. During 24 h of time-on-stream, ethanol was completely converted and the carbon formation rate increased of only 4 times (3.1 vs 12.5 $g_c/(g_{c,f}*g_{cat}*h)$) with respect to the impurity-free case. Finally, the comparison with literature data highlighted the promising performances, in terms of reduced carbon selectivity, of the Pt-Ni catalyst supported on ceria-zirconia.

References

Ay H., Üner D., 2015, Dry reforming of methane over CeO$_2$ supported Ni, Co and Ni–Co catalysts. Appl. Catal. B: Environ., 179, 128–138.

Kiss A.A., Suszwalak D. J-P., 2012, Enhanced bioethanol dehydration by extractive and azeotropic distillation in dividing-wall columns., Sep. Purif. Technol., 86, 70-78.

Koo K. Y., Lee J. H., Jung U. H., Kim S. H., Yoon W. L., 2015, Combined H$_2$O and CO$_2$ reforming of coke oven gas over Ca-promoted Ni/MgAl2O4 catalyst for direct reduced iron production. Fuel, 153, 303-309.

Le Valant A., Bion N., Fabien Can F., Duprez D., Epron F., 2010a, Preparation and characterization of bimetallic Rh-Ni/Y$_2$O$_3$-Al$_2$O$_3$ for hydrogen production by raw bioethanol steam reforming: influence of the addition of nickel on the catalyst performances and stability, Appl. Catal. B: Environ., 97, 72-81.

Le Valant A., Can F., Bion N., Duprez D., Epron F., 2010b, Hydrogen production from raw bioethanol steam reforming: Optimization of catalyst composition with improved stability against various impurities, Int. J. Hydrogen Energ., 35, 5015-5020.

Le Valant A., Garron A., Bion N., Duprez D., Epron F., 2011, Effect of higher alcohols on the performances of a 1%Rh/MgAl2O4/Al2O3 catalyst for hydrogen production by crude bioethanol steam reforming, Int. J. Hydrogen Energ., 36, 311-318.

Mondal T., Pant K. K., Dalai A. K., 2015, Oxidative and non-oxidative steam reforming of crude bio-ethanol for hydrogen production over Rh promoted Ni/CeO$_2$-ZrO$_2$ catalyst, Appl. Catal. A: Gen., 499, 19–31.

Moretti E., Storaro L., Talon A., Chitsazan S., Garbarino G., Busca G., Finocchio E., 2015, Ceria–zirconia based catalysts for ethanol steam reforming, Fuel, 153, 166-175.

Ni M., Leung D.Y.C., Leung M.K.H., 2007, A review on reforming bio-ethanol for hydrogen production, Int. J. Hydrogen Energ., 32, 3238–3247.

Palma V., Castaldo F., Ciambelli P., Iaquaniello G., 2014, CeO$_2$-supported Pt/Ni catalyst for the renewable and clean H2 production via ethanol steam reforming. Appl. Catal. B: Environ., 145, 73-84.

Palma V., Castaldo F., Ciambelli P., Iaquaniello G., 2012, Bio-ethanol steam reforming reaction over bimetallic ceria-supported catalysts. Chem. Eng. Trans., 29, 109-114.

Rass-Hansen J., Johansson R., Møller M., 2008, Christensen C. H., Steam reforming of technical bioethanol for hydrogen production, Int. J. Hydrogen Energ., 33, 4547-4554.

Romero-Sarria F., Vargas J.C., Roger A-C, Kiennemann A., 2008, Hydrogen production by steam reforming of ethanol: Study of mixed oxide catalysts Ce$_2$Zr$_{1.5}$Me$_{0.5}$O$_8$: Comparison of Ni/Co and effect of Rh. Catal. Today, 133, 149-153.

Shao S., Shi A.-W., Liu C.-L., Yang R.-Z., Dong W.-S., 2014, Hydrogen production from steam reforming of glycerol over Ni/CeZrO catalysts. Fuel Process. Technol.,125, 1–7.

Sheikh M., Abbas Z., 2015, Homogeneous–heterogeneous reactions in stagnation point flow of Casson fluid due to a stretching/shrinking sheet with uniform suction and slip effects. Ain Shams Engineering Journal, <www.sciencedirect.com/science/article/pii/S2090447915001677>

Styarini D., Aristiawan Y., Abimanyu H., Sudiyani Y., 2013, Determination of Organic Impurities in Lignocellulosic Bioethanol Product by GC-FID. Energy Procedia, 32,153-159.

Zhu Q., Cheng H., Zou X., Lu X., Xu Q., Zhou Z., 2015, Synthesis, characterization, and catalytic performance of La$_{0.6}$Sr$_{0.4}$Ni$_x$Co$_{1-x}$O$_3$ perovskite catalysts in dry reforming of coke oven gas. Chinese J. Catal., 39, 915-924.